Netherlands
organization for
applied scientific
research

FEL

TNO Physics and Electronics
Laboratory

P.O. Box 96864
2509 JG The Hague
Oude Waalsdorperweg 63
The Hague, The Netherlands

Fax +31 70 328 09 61
Phone +31 70 326 42 21

TNO-report

report no. FEL-90-A112

copy no. 7

title

Frequency-domain analysis of one-dimensional electromagnetic scattering by lossy media

author(s):

Ir. J.J.A. Klaasen

classification	
title	: unclassified
abstract	: unclassified
report	: unclassified
no. of copies	: 20
no. of pages	: 42
appendices	: -
date	: May 1990

All information which is classified according to Dutch regulations shall be treated by the recipient in the same way as classified information of corresponding value in his own country. No part of this information will be disclosed to any party.

TNO

report no. : FEL-90-A112
title : Frequency-domain analysis of one-dimensional electromagnetic scattering by lossy media

author(s) : Ir. J.J.A. Klaasen
institute : TNO Physics and Electronics Laboratory

date : May 1990
NDRO no. : A86K012
no. in pow '90 : 714.1

ABSTRACT (UNCLASSIFIED)

A study was performed to investigate the effect of a plane interface between two media with different electromagnetic properties, on the electromagnetic fields. Such an interface exists between e.g. an air/earth or air/water boundary. This report presents the results of this study.
The incident field is assumed to be a uniform plane wave. Therefore this study adresses the one-dimensional scattering problem. The analysis is performed in the s-domain, i.e. using the Laplace transform.
Numerical results are presented for the scattering of a NEMP by the earth's surface and the sea.

rapport no. : FEL-90-A112
titel : Analyse van het één-dimensionale verstoringsprobleem aan een medium met verliezen in het frequentiedomein

auteur(s) : Ir. J.J.A. Klaasen
instituut : Fysisch en Elektronisch Laboratorium TNO

datum : mei 1990
hdo-opdr.no. : A86K012
no. in iwp '90 : 714.1

SAMENVATTING (ONGERUBRICEERD)

Een studie is verricht naar de invloed van een grensvlak tussen twee media met verschillende elektromagnetische eigenschappen, op de elektromagnetische velden. Zo'n grensvlak bestaat bijvoorbeeld tussen lucht en aarde, of lucht en water. Dit rapport geeft de resultaten van deze studie weer.
Voor deze studie wordt er vanuit gegaan dat het invallende veld een uniforme vlakke golf is. Dus, dit rapport behandelt het één-dimensionale verstrooiingsprobleem. De analyse is uitgevoerd in het s-domein (Laplace transformatie).
Numerieke resultaten worden gepresenteerd van de verstrooiing van een NEMP aan het aard- en het zee-oppervlak.

1 INTRODUCTION

In most electromagnetic scattering configurations the influence of the earth has to be taken into account, because an object in the vicinity of the earth's surface is not only irradiated by the incident field, but also by the field reflected by the earth. Such scattering configurations occur in Nuclear ElectroMagnetic Pulse (NEMP) interaction studies, which are conducted by the EMP-group of the Physics and Electronics Laboratory of TNO (FEL-TNO).
Therefore a study was performed to investigate the effect of a plane interface between two media with different electromagnetic properties, on the electromagnetic fields. Such an interface exists between e.g. an air/earth or air/water boundary. This report presents the results of this study.

In Chapter 2 the formulation of the problem is presented in the s-domain, i.e. using the Laplace transform, for horizontally and vertically polarized incident electromagnetic fields.
In Chapter 3 some properties of the reflected and refracted fields are discussed, while some useful approximations are presented in Chapter 4. In Chapter 5 some numerical results are presented for the scattering of a Nuclear ElectroMagnetic Pulse (NEMP) by the earth's surface and the sea.
Finally, some conclusions are drawn in Chapter 6.

2 DESCRIPTION AND SOLUTION OF THE ELECTROMAGNETIC SCATTERING PROBLEM IN THE S-DOMAIN

In section 2.1 the scattering configuration is defined, while in sections 2.2 and 2.3 the scattering problem is solved for vertically and horizontally polarized fields, respectively.

2.1 Description of the scattering configuration

The one-dimensional scattering configuration depicted in fig. 2.1 is considered. To specify the position in this unbounded space, we employ the coordinates (x, y, z) with respect to a given orthogonal right-handed Cartesian reference frame with origin O. The unit vectors along the axes are denoted by $\underline{i}_x$, $\underline{i}_y$ and $\underline{i}_z$. Then the position vector in this coordinate system is given by

$$\underline{r} = x\underline{i}_x + y\underline{i}_y + z\underline{i}_z. \tag{2.1}$$

The time coordinate is denoted by t, and the s-domain quantities are obtained by applying the Laplace transform with respect to time. The Laplace transform is defined by

$$\mathcal{L}\{f(t)\} = \hat{f}(s) = \int_0^\infty e^{-st} f(t)\, dt, \tag{2.2}$$

and the inverse Laplace transform is given by

$$f(t) = \frac{1}{2\pi i} \int_{\gamma-i\infty}^{\gamma+i\infty} e^{st} \hat{f}(s)\, ds, \tag{2.3}$$

where i is the imaginary unit. The integration for the inverse Laplace transform is performed along the Bromwitch contour, LePage [1], with γ a positive real number. In eq.(2.3), γ is chosen such that $\exp(-\gamma t)\,|f(t)| < M$, where M is a finite positive real number.

Furthermore, let the half-space $\mathcal{D}_1$ be given by

$$\mathcal{D}_1 = \{ x, y, z \in \mathbb{R} \mid z < 0 \}, \tag{2.4}$$

and let the half-space $\mathcal{D}_2$ be given by

$$\mathcal{D}_2 = \{ x, y, z \in \mathbb{R} \mid z > 0 \}. \tag{2.5}$$

This configuration is irradiated by an incident uniform electromagnetic plane wave. The source, which generates the incident field, is located in $\mathcal{D}_1$. The constitutive constants of the half-space $\mathcal{D}_1$ are assumed to be those of vacuum, i.e. ϵ_0 and μ_0. The half-space $\mathcal{D}_2$ is assumed to consist of homogeneous, isotropic, time-invariant, linear and instantaneous and locally reacting material. The material in $\mathcal{D}_2$ is characterized in its electromagnetic behavior by the permittivity ϵ, the permeability μ, and the conductivity σ. Furthermore there are no sources present in $\mathcal{D}_2$.

The incident uniform electromagnetic plane wave propagates in the direction of the propagation vector $\underline{\chi}_i$. The propagation vector $\underline{\chi}_i$ is of unit length and makes an angle φ_i with the normal $\underline{n}$ on the plane interface between the two media, directing inwards $\mathcal{D}_2$, and with $\varphi_i < 90^\circ$.

This configuration allows the waves to propagate in two independent ways, in which any incident wave can be decomposed. To the horizontal component of the incident magnetic field one can apply a coordinate transformation such that this component runs parallel to one of the horizontal axis. This component is referred to as the TM-mode. The horizontal component of the incident electric field can be treated in the same way. The wave propagation in this case is referred to as the TE-mode. It can be proven easily that any incident plane wave can be written as a linear combination of these two kinds of wave propagation. Therefore, we shall solve these two independent kinds of wave

propagation in the next sections.

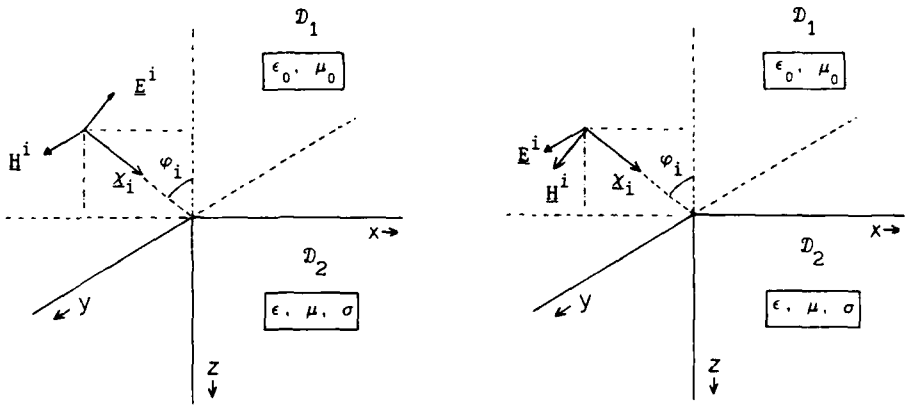

Fig. 2.1. Electromagnetic scattering configuration.
a) vertically polarized field,
b) horizontally polarized field.

2.2 Vertically polarized incident field

Let the incident magnetic field be a uniform plane wave, and let it have an y-component only (TM-mode). Furthermore, the incident field hits the interface between $\mathcal{D}_1$ and $\mathcal{D}_2$ at t = 0. Then the incident magnetic field is given by

$$\hat{H}_y^i(\underline{r},s) = \hat{H}_0(s)\, e^{-\gamma_0(\underline{\chi}_i \cdot \underline{r})}, \qquad \underline{r} \in \mathcal{D}_1 \tag{2.6}$$

with the propagation vector $\underline{\chi}_i$ given by

$$\underline{\chi}_i = \sin\varphi_i \underline{i}_x + \cos\varphi_i \underline{i}_z. \tag{2.7}$$

In eq.(2.6), the propagation constant γ_0 is given by

$$\gamma_0 = s\,(\epsilon_0\mu_0)^{1/2} = \frac{s}{c_0}, \tag{2.8}$$

where c_0 denotes the speed of light in vacuum. $\hat{H}_0(s)$ denotes the Laplace transformed wave form of the incident magnetic field.
Substitution of $\underline{x}_i$ in eq.(2.6) yields

$$\hat{H}^i_y = \hat{H}_0 e^{-\gamma_0(x \sin\varphi_i + z\cos\varphi_i)}, \qquad \underline{r} \in \mathcal{D}_1 \tag{2.9}$$

which represents a wave propagating in the positive x- and z-direction. The incident electric field is given by

$$\begin{aligned} \hat{E}^i_x(\underline{r},s) &= \cos\varphi_i\, Z_0 \hat{H}^i_y, \\ \hat{E}^i_z(\underline{r},s) &= -\sin\varphi_i\, Z_0 \hat{H}^i_y, \end{aligned} \qquad \underline{r} \in \mathcal{D}_1 \tag{2.10}$$

where Z_0 denotes the wave impedance of vacuum and is given by

$$Z_0 = \hat{E}_0/\hat{H}_0 = \left(\frac{\mu_0}{\epsilon_0}\right)^{1/2}. \tag{2.11}$$

The reflected fields in $\mathcal{D}_1$ propagate in the direction of the propagation vector $\underline{x}_r = \sin\varphi_i \underline{i}_x - \cos\varphi_i \underline{i}_z$. Since the scattering process is independent on the spatial variables (x, y), the reflected fields in $\mathcal{D}_1$ are given by

$$\hat{H}^r_y(\underline{r},s) = \hat{R}^H \hat{H}_0 e^{-\gamma_0(\underline{x}_r\cdot\underline{r})} = \hat{R}^H \hat{H}_0 e^{-\gamma_0(x\sin\varphi_i - z\cos\varphi_i)},$$

$$\begin{aligned} \hat{E}^r_x(\underline{r},s) &= -\cos\varphi_i\, Z_0 \hat{H}^r_y, \\ \hat{E}^r_z(\underline{r},s) &= -\sin\varphi_i\, Z_0 \hat{H}^r_y, \end{aligned} \qquad \underline{r} \in \mathcal{D}_1 \tag{2.12}$$

which are uniform plane waves. In eq.(2.12) we have used the fact that the angle of incidence equals the angle of reflection. $\hat{R}^H$ denotes the TM-mode reflection coefficient which must be determined from the boundary conditions at the plane interface. $\hat{R}^H$ is given by the ratio of the reflected and incident magnetic field at the plane interface, i.e. $\hat{R}^H = \lim_{z \uparrow 0} \hat{H}_y^r / \hat{H}_y^i$. The expressions for the electric fields in eq.(2.12) are obtained after substitution of the reflected magnetic field in Maxwell's equations.

From the one-dimensional wave equation the propagation constant γ in $\mathcal{D}_2$ is found to be

$$\gamma = \|\underline{\gamma}\| = (s\mu(s\epsilon + \sigma))^{1/2} , \tag{2.13}$$

where

$$\underline{\gamma} = \gamma_x \underline{i}_x + \gamma_z \underline{i}_z . \tag{2.14}$$

The transmitted waves in $\mathcal{D}_2$ are in general non-uniform plane waves. The fields in $\mathcal{D}_1$ and $\mathcal{D}_2$ can only couple when γ_x in $\mathcal{D}_1$ equals γ_x in $\mathcal{D}_2$ $\forall\, x \in \mathbb{R}$. Hence, we must also have in $\mathcal{D}_2$

$$\gamma_x = \gamma_0 \sin \varphi_i . \tag{2.15}$$

The transmitted waves can be represented as

$$\begin{aligned} \hat{H}_y^t(\underline{r},s) &= \hat{T}^H \hat{H}_0 e^{-(\underline{\gamma}\cdot\underline{r})} = \hat{T}^H \hat{H}_0 e^{-(x\gamma_x + z\gamma_z)} , \\ \hat{E}_x^t(\underline{r},s) &= Z_t \hat{H}_y^t , \qquad \underline{r} \in \mathcal{D}_2 \\ \hat{E}_z^t(\underline{r},s) &= -Z_n \hat{H}_y^t , \end{aligned} \tag{2.16}$$

where $\hat{T}^H$ denotes the TM-mode transmission coefficient, which must also be determined from the boundary conditions at the plane interface. $\hat{T}^H$

gives the ratio between the transmitted and incident magnetic field at the plane interface, i.e. $\hat{T}^H = \lim_{z\downarrow 0} \hat{H}_y^t / \hat{H}_y^i$. Z_n and Z_t denote the normal and transverse wave impedances, respectively. The latter is also known as the surface impedance, Wait [2]. Both are found from a direct substitution of the transmitted magnetic field of eq.(2.16) in Maxwell's equations. After doing so, we obtain

$$Z_t = \frac{\gamma_z}{s\epsilon + \sigma},$$
$$Z_n = \frac{\gamma_x}{s\epsilon + \sigma}. \tag{2.17}$$

The propagation constant in the z-direction is found from eqs.(2.13) and (2.14), and is given by

$$\gamma_z = \sqrt{\gamma^2 - \gamma_x^2}, \qquad \mathrm{Re}(\gamma_z) \geq 0, \tag{2.18}$$

where γ is given by eq.(2.13), and γ_x by eq.(2.15). Since the transmitted wave in $\mathcal{D}_2$ must obey the radiation condition at $z \to \infty$, we must select that branch of γ_z where the real part of γ_z is positive.

As mentioned before the transmission and reflection coefficients follow from the boundary conditions for the tangential electric and magnetic fields, which state

$$\lim_{z\uparrow 0} \hat{H}_y^i + \hat{H}_y^r = \lim_{z\downarrow 0} \hat{H}_y^t,$$
$$\lim_{z\uparrow 0} \hat{E}_x^i + \hat{E}_x^r = \lim_{z\downarrow 0} \hat{E}_x^t. \tag{2.19}$$

After substitution of the relevant equations in eq.(2.19), we obtain

$$\hat{R}^H = \frac{Z' - 1}{Z' + 1}, \qquad \hat{T}^H = \frac{2Z'}{Z' + 1}, \tag{2.20}$$

where

$$Z' = \frac{Z_0 \cos \varphi_i}{Z_t} = \frac{\eta^2 \cos \varphi_i}{\mu_r \sqrt{\eta^2 - \sin^2 \varphi_i}}, \tag{2.21}$$

and where η denotes the index of refraction given by

$$\eta = \frac{\gamma}{\gamma_0} = \sqrt{\epsilon_r \mu_r \left(\frac{\sigma}{s\epsilon} + 1\right)}. \tag{2.22}$$

Observe that $Z_0 \cos \varphi_i$ corresponds to the surface impedance of the medium in $\mathcal{D}_1$, so that Z' is the quotient between the surface impedances of the media in $\mathcal{D}_1$ and $\mathcal{D}_2$.

2.3 Horizontally polarized incident field

Let the incident electric field be a uniform plane wave, and let it have an y-component only (TE-mode). Again, the incident field hits the interface between $\mathcal{D}_1$ and $\mathcal{D}_2$ at $t = 0$. Then the incident electric field is represented by

$$\hat{E}^i_y(\underline{r}, s) = \hat{E}_0(s)\, e^{-\gamma_0 (\underline{x}_i \cdot \underline{r})}, \qquad \underline{r} \in \mathcal{D}_1 \tag{2.23}$$

with $\underline{x}_i$ given by eq.(2.7), and γ_0 given by eq.(2.8). $\hat{E}_0(s)$ denotes the Laplace transformed wave form of the incident electric field. From

Maxwell's equations we obtain for the incident magnetic field

$$\begin{aligned} \hat{H}_x^i(\underline{r},s) &= -\cos\varphi_i \; Y_0 \hat{E}_y^i, \\ \hat{H}_z^i(\underline{r},s) &= \sin\varphi_i \; Y_0 \hat{E}_y^i, \end{aligned} \qquad \underline{r} \in \mathcal{D}_1 \tag{2.24}$$

where Y_0 denotes the wave admittance of vacuum, and is given by

$$Y_0 = \hat{H}_0/\hat{E}_0 = \left(\frac{\epsilon_0}{\mu_0}\right)^{1/2}. \tag{2.25}$$

With the same reasoning as in section 2.2, the reflected waves in $\mathcal{D}_1$ are given by

$$\begin{aligned} \hat{E}_y^r(\underline{r},s) &= \hat{R}^E \hat{E}_0 e^{-\gamma_0(\underline{x}_r\cdot\underline{r})} = \hat{R}^E \hat{E}_0 e^{-\gamma_0(x\sin\varphi_i - z\cos\varphi_i)}, \\ \hat{H}_x^r(\underline{r},s) &= \cos\varphi_i \; Y_0 \hat{E}_y^r, \\ \hat{H}_z^r(\underline{r},s) &= \sin\varphi_i \; Y_0 \hat{E}_y^r, \end{aligned} \qquad \underline{r} \in \mathcal{D}_1 \tag{2.26}$$

where $\hat{R}^E$ denotes the TE-mode reflection coefficient, which is given by the ratio of the reflected and the incident electric field at the plane interface, i.e. $\hat{R}^E = \lim_{z\uparrow 0} \hat{E}_y^r / \hat{E}_y^i$.
The transmitted waves for the TE-mode are non-uniform plane waves, and are represented by

$$\begin{aligned} \hat{E}_y^t(\underline{r},s) &= \hat{T}^E \hat{E}_0 e^{-(\underline{\gamma}\cdot\underline{r})} = \hat{T}^E \hat{E}_0 e^{-(x\gamma_x + z\gamma_z)}, \\ \hat{H}_x^t(\underline{r},s) &= -Y_t \hat{E}_y^t, \\ \hat{H}_z^t(\underline{r},s) &= Y_n \hat{E}_y^t, \end{aligned} \qquad \underline{r} \in \mathcal{D}_2 \tag{2.27}$$

where $\hat{T}^E$ denotes the TE-mode transmission coefficient given by the ratio

of the transmitted and incident electric field, i.e. $\hat{T}^E = \lim_{z \downarrow 0} \hat{E}_y^t / \hat{E}_y^i$. Y_n and Y_t denote the normal and transverse (or surface) wave admittances, respectively. Both are found from a direct substitution of the transmitted electric field of eq.(2.27) in Maxwell's equations. After doing so, we obtain for the admittances

$$Y_t = \frac{\gamma_z}{s\mu},$$
$$Y_n = \frac{\gamma_x}{s\mu}. \tag{2.28}$$

Again applying the boundary conditions, we obtain for the TE-mode reflection and transmission coefficients

$$\hat{R}^E = \frac{Y' - 1}{Y' + 1},$$
$$\hat{T}^E = \frac{2Y'}{Y' + 1}, \tag{2.29}$$

where

$$Y' = \frac{Y_0 \cos \varphi_i}{Y_t} = \frac{\mu_r \cos \varphi_i}{\sqrt{\eta^2 - \sin^2 \varphi_i}}. \tag{2.30}$$

Notice that Y' denotes the ratio between the surface admittances of the media in $\mathcal{D}_1$ and $\mathcal{D}_2$.

3 PROPERTIES OF THE FIELDS

Some properties of the reflected and transmitted waves, which will clarify some of the properties of wave propagation in the frequency domain, are discussed in this chapter. The expressions in the s-domain are transformed to the frequency domain because of the physical importance of the frequency domain. This is simply done by replacing s by $i\omega$.

3.1 Propagation of the transmitted fields

First of all let us define the quantities v and φ_t. If the medium in $\mathcal{D}_2$ is lossless, the transmitted waves propagate with speed v given by

$$v = \frac{1}{\sqrt{\epsilon\mu}} . \tag{3.1}$$

Also for the lossless case, the propagation vector of the transmitted wave $\underline{x}_t = \sin\varphi_t \underline{i}_x + \cos\varphi_t \underline{i}_z$ makes an angle φ_t with the z-axis, where

$$\cos\varphi_t = \sqrt{1 - \frac{v^2}{c_0^2}\sin^2\varphi_i} . \tag{3.2}$$

After rewriting the propagation factor in $\mathcal{D}_2$ in the frequency domain, and using eqs.(3.1)-(3.2), the propagation factor is written as

$$e^{-(x\gamma_x + z\gamma_z)} = e^{-i(xk_x + zk_z)}, \qquad \underline{r} \in \mathcal{D}_2 \tag{3.3}$$

where

$$k_x = -i\gamma_x = -i\gamma_0 \sin\varphi_i = k_0 \sin\varphi_i, \tag{3.4}$$

and

$$k_z = -i\gamma_z = \sqrt{\eta^2 - \sin^2\varphi_i}\; k_0 = \frac{\omega}{v}\cos\varphi_t \sqrt{1 - i\frac{\sigma}{\omega\epsilon\cos^2\varphi_t}}\,. \tag{3.5}$$

In eqs.(3.4)-(3.5) k_0 denotes the wave number of vacuum and is given by ω/c_0. Furthermore, the square root in eq.(3.5) must be chosen such, that $\mathrm{Im}(k_z) \leq 0$.
As mentioned earlier, the transmitted waves in $\mathcal{D}_2$, for both TM- and TE-mode, are non-uniform waves due to losses of the medium in $\mathcal{D}_2$. While the transmitted fields propagate in the positive z-direction, they are attenuated. This can be seen easily when the wave number k_z in $\mathcal{D}_2$ is decomposed in its real and imaginary part. After doing so the propagation factor is rewritten as

$$e^{-i(xk_x + zk_z)} = e^{zk_z''}\, e^{-i(xk_x + zk_z')}, \tag{3.6}$$

where k_z' denotes the real and k_z'' the imaginary part of k_z. Both are given by

$$k_z' = \frac{\omega}{v}\cos\varphi_t \left[\frac{1}{2}\sqrt{1 + \left(\frac{\sigma}{\omega\epsilon\cos^2\varphi_t}\right)^2} + \frac{1}{2}\right]^{1/2},$$

$$k_z'' = -\frac{\omega}{v}\cos\varphi_t \left[\frac{1}{2}\sqrt{1 + \left(\frac{\sigma}{\omega\epsilon\cos^2\varphi_t}\right)^2} - \frac{1}{2}\right]^{1/2}. \tag{3.7}$$

Planes of equal amplitude are given by z = constant, while planes of equal phase are given by the equation $xk_x + zk_z'$ = constant. See fig. 3.1.

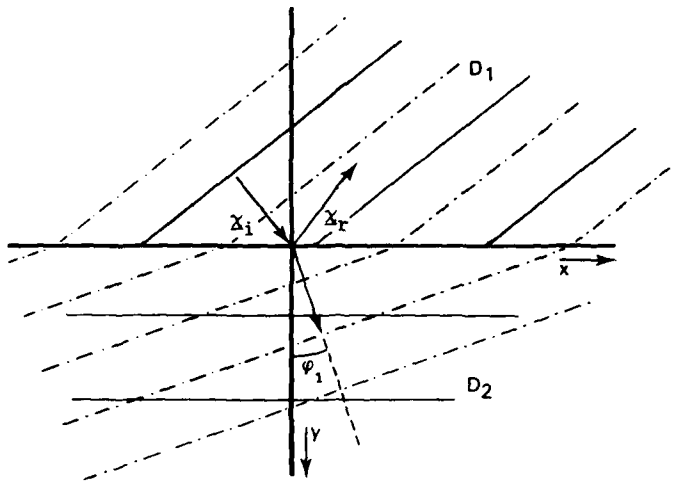

Fig. 3.1. Planes of constant amplitude (——) and of constant phase (- - -)

When the angle between the normal of the planes of equal phase and the normal of the planes of equal amplitude is denoted by φ_1, the phase factor of the propagation factor can be written as

$$e^{-i(xk_x + zk'_z)} = e^{-i(xk_0 \sin\varphi_i + zk_1 \cos\varphi_1)}, \tag{3.8}$$

with

$$k_1 = \sqrt{k_x^2 + k_z'^2}\,,$$
$$\cos\varphi_1 = \sqrt{1 - \frac{k_0^2}{k_1^2}\sin^2\varphi_i}\,. \tag{3.9}$$

Notice that φ_1 is frequency-dependent. With this notation we can

formulate Snell's law for lossy media, which is then given by

$$k_1 \sin \varphi_1 = k_0 \sin \varphi_i, \tag{3.10}$$

where φ_1 can be interpreted as the angle between the propagation vector of the transmitted field and the positive z-axis (see fig.3.1). Using eq.(3.10) the phase factor can be rewritten as

$$e^{-i(xk_x + zk_z')} = e^{-ik_1(x \sin \varphi_i + z \cos \varphi_1)}, \tag{3.11}$$

Notice that if the conductivity σ vanishes, φ_1 equals φ_t and eq.(3.10) results in Snell's law for lossless media.
A very well-known property with respect to wave propagation in lossy media, is the skin depth. It denotes that depth $z = \delta$, for which the amplitude has been attenuated by a factor e^{-1}. It then follows from eq.(3.6) that the skin depth δ is given by

$$\delta = -\frac{1}{k_z''}, \tag{3.12}$$

with k_z'' given by eq.(3.7).
The attenuation α in dB's per meter follows also from eq.(3.6) and is given by

$$\alpha = -8.686\, k_z''. \tag{3.13}$$

3.2 Brewster angle

The Brewster angle is the angle of incidence for which there are no reflected fields. For vertical polarization, we observe from eq.(2.20) that the Brewster angle occurs if $Z' = 1$, i.e. there is a match between the surface impedances of the media in $\mathcal{D}_1$ and $\mathcal{D}_2$. The electromagnetic energy is then completely transported into $\mathcal{D}_2$. Z' is given by eq.(2.21).

Therefore, the condition to be satisfied is

$$\frac{\eta^2 \cos \varphi_i}{\mu_r \sqrt{\eta^2 - \sin^2 \varphi_i}} = 1. \tag{3.14}$$

If only real angles of incidence are allowed, i.e. the incident wave is uniform, this condition can only be satisfied when the imaginary part of η^2 vanishes. This occurs when the medium in $\mathcal{D}_2$ is lossless. Hence from eq.(3.14) with $\sigma = 0$, we find for the sine of the Brewster angle φ_b^H

$$\sin \varphi_b^H = \sqrt{\frac{\epsilon_r(\epsilon_r - \mu_r)}{\epsilon_r^2 - 1}}\ . \tag{3.15}$$

Notice that the Brewster angle exists only if $\epsilon_r \geq \mu_r$.
For the special case $\mu = \mu_0$ eq.(3.15) simplifies to

$$\sin \varphi_b^H = \sqrt{\frac{\epsilon_r}{\epsilon_r + 1}}\ . \tag{3.16}$$

Since $\epsilon_r > 1$, it follows from eq.(3.16) that if $\mu = \mu_0$ then $\varphi_b^H > 45^\circ$.
It can be shown that the dielectric reflection coefficient is positive for angles of incidence smaller than the Brewster angle, and negative for angles of incidence larger than the Brewster angle.
The situation $R^H = 0$ in the lossless case can be seen as a special case of the lossy case, but then with the condition that R^H has a minimum. It is then customary to speak of the pseudo Brewster angle. The pseudo Brewster angle is frequency-dependent, and exists only if the angle of incidence is larger than the Brewster angle.
Fig.3.2 shows the modulus of the reflection coefficient as a function of the angle of incidence for an air/earth and air/sea water interface.

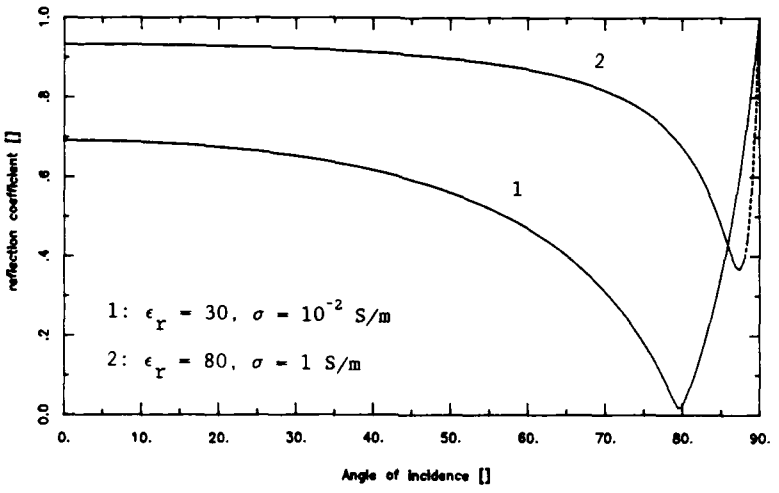

Fig.3.2. Modulus of the reflection coefficient as a function of the angle of incidence for an air/earth $\epsilon_r = 30$ and $\sigma = 10^{-2}$ S/m (clay), with $\varphi_b^H = 79.7^\circ$, and air/sea water interface $\epsilon_r = 80$ and $\sigma = 1$ S/m, with $\varphi_b^H = 83.6^\circ$. $\omega = 2\pi \cdot 100 \times 10^6$ and $\mu_r = 1$.

If the angle of incidence equals the Brewster angle, the high-frequency components are not reflected, because then the reflection coefficient vanishes. In those cases that the angle of incidence deviates from the Brewster angle, the reflection coefficient reduces to the high-frequency limit. It will be shown in Chapter 4 that this limit is the dielectric reflection coefficient, i.e. the reflection coefficient with zero conductivity.

Figs. 3.3a, b and c, show some of the above mentioned properties.

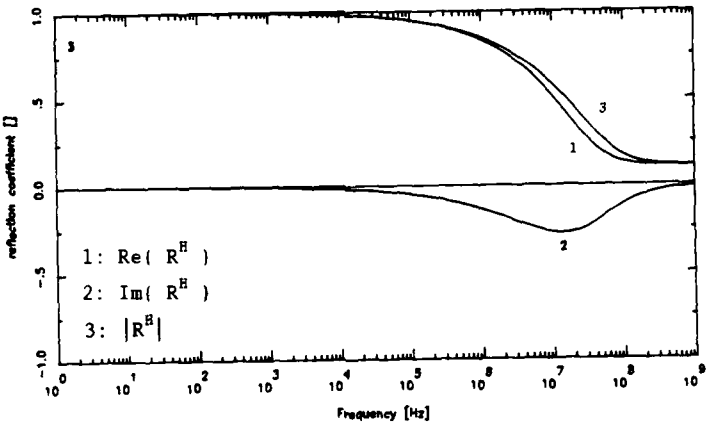
reflection coefficient []
1.0
.5
0.0
-.5
-1.0
1: Re(R^H)
2: Im(R^H)
3: |R^H|
Frequency [Hz]

(a)

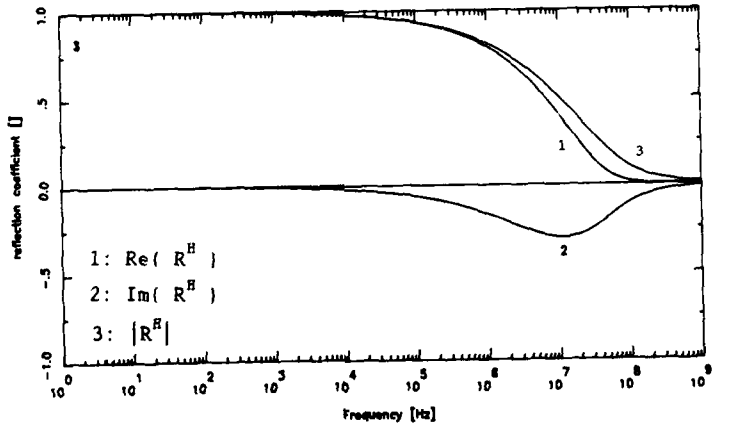
reflection coefficient []
1.0
.5
0.0
-.5
-1.0
1: Re(R^H)
2: Im(R^H)
3: |R^H|
Frequency [Hz]

(b)

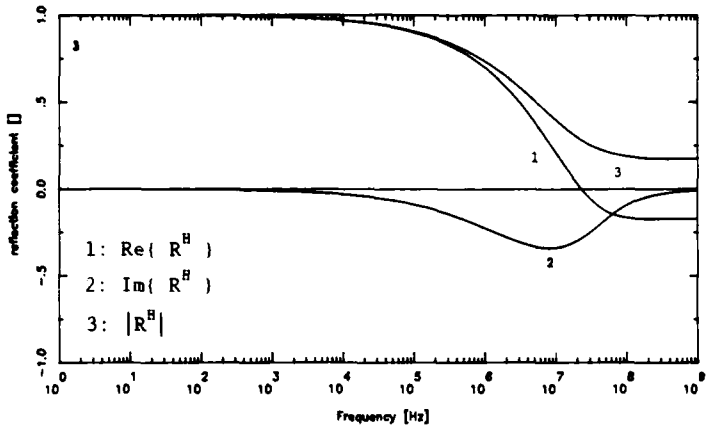

(c)

Fig.3.3. Reflection coefficient as a function of frequency. Brewster angle $\varphi_b^H = 60^\circ$, $\epsilon_r = 3$, $\mu_r = 1$, $\sigma = 10^{-2}$ (dry soil).
a) $\varphi_i = 50^\circ$,
b) $\varphi_i = 60^\circ$,
c) $\varphi_i = 70^\circ$.

Fig.3.3a shows the reflection coefficient as a function of frequency if the angle of incidence is smaller than the Brewster angle. Fig.3.3b shows the reflection coefficient if the angle of incidence is equals the Brewster angle, and fig.3.3c if the angle of incidence is larger than the Brewster angle. In all cases the Brewster angle $\varphi_b^H = 60^\circ$.

If the incident electric field is horizontal polarized a similar phenomena like the above described Brewster angle can occur. The condition to be satisfied is then given by

$$\mu_r \cos \varphi_i = \sqrt{\epsilon_r \mu_r - \sin^2 \varphi_i}, \qquad (3.17)$$

which yields for the Brewster angle for horizontal polarization

$$\sin \varphi_b^E = \sqrt{\frac{\mu_r(\mu_r - \epsilon_r)}{\mu_r^2 - 1}} \quad . \tag{3.18}$$

Notice that the Brewster angle φ_b^E exists only if $\mu_r \geq \epsilon_r$.
In most practical applications $\mu_r = 1$. Consequently, the Brewster angle for horizontal polarization does not occur.

4 USEFUL APPROXIMATIONS

In some practical cases useful approximations can be made, that reduce the complexity of the equations given in the previous chapters. Two kind of approximations can be made :

- Low-frequency/high-loss approximation,
- High-frequency/low-loss approximation.

These approximations will be presented in the next two sections.

4.1 Low-frequency/high-loss approximation

For the special case that the spectrum of the incident field contains low frequencies only, some useful approximations can be made. We start with approximating the index of refraction given by eq.(2.22). Now if $\frac{\sigma}{\omega\,\epsilon} \gg 1$, η can be rewritten as

$$\eta \approx \sqrt{\frac{\mu_r \sigma}{2\omega\epsilon_0}}\,(1-i). \tag{4.1}$$

If $\frac{\sigma}{\omega\,\epsilon} \gg 1$, we certainly have that $\frac{\sigma}{\omega\,\epsilon} \gg 1 - \frac{1}{\epsilon_r \mu_r}\sin^2\varphi_i$. Then k_z is approximated by (cf. eq.(3.5))

$$k_z \approx \eta\, k_0 = \sqrt{\frac{\mu\sigma\omega}{2}}\,(1-i), \tag{4.2}$$

where we have used η given by eq.(4.1). From eq.(3.12) together with eq.(4.2), we find for the skin depth

$$\delta \approx \sqrt{\frac{2}{\mu\sigma\omega}}. \tag{4.3}$$

Fig. 4.1 shows some typical values for the skin depth, with $\mu = \mu_0$.

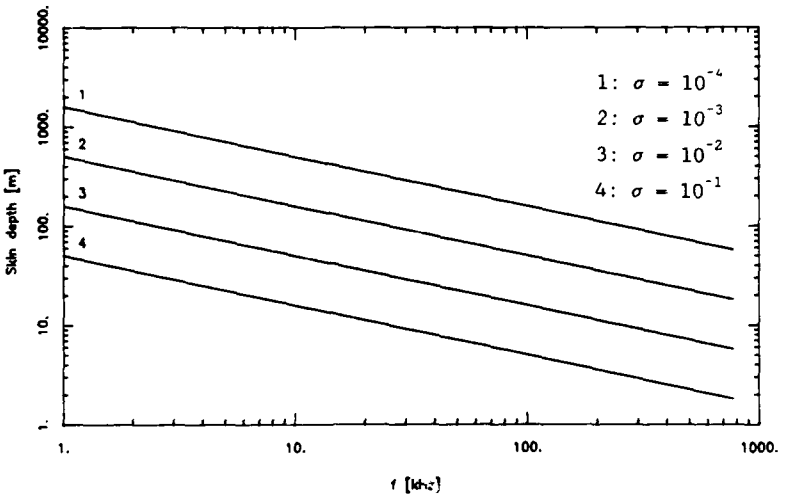

Fig 4.1. Skin depth for various conductivities with $\mu = \mu_0$ (low-frequency/high-loss approximation).

From fig. 4.1, we can conclude that the low-frequency components of the transmitted waves in $\mathcal{D}_2$, can travel large distances without significant attenuation.
Also using the low-frequency approximation, k_1 is approximated by

$$k_1 \approx \eta' k_0, \tag{4.4}$$

where η' denotes the real part of η given by eq.(4.1). From Snell's law, it then follows that

$$\sin \varphi_1 = \frac{1}{\eta'} \sin \varphi_i \approx 0, \tag{4.5}$$

which implies that $\varphi_1 \approx 0$. From this we can conclude that for low frequencies the transmitted waves propagate almost entirely in the

direction of the positive z-axis.

The low-frequency approximation can also be applied successfully to the expressions for the reflection and transmission coefficients. We do so by approximating Z' and Y' first. After substitution of eq.(4.1) in eqs.(2.21) and (2.30), we obtain

$$Z' \approx \frac{\eta \cos \varphi_i}{\mu_r},$$
$$Y' \approx \frac{\mu_r \cos \varphi_i}{\eta}, \tag{4.6}$$

with η again given by eq.(4.1). The reflection and transmission coefficients for a vertically polarized incident field then simplify to

$$\hat{R}^H \approx \frac{\eta \cos \varphi_i - \mu_r}{\eta \cos \varphi_i + \mu_r},$$
$$\hat{T}^H \approx \frac{2\eta \cos \varphi_i}{\eta \cos \varphi_i + \mu_r}. \tag{4.7}$$

For very-low frequencies and for angles of incidence not near the Brewster angle (which is slightly less than 90° in this case), $Z' \gg 1$. Therefore $\hat{R}^H \approx 1$, and $\hat{T}^H \approx 2$.
After substitution of the approximated Y' in the expressions for the reflection and transmission coefficients for a horizontal polarization, we obtain

$$\hat{R}^E \approx \frac{\mu_r \cos \varphi_i - \eta}{\mu_r \cos \varphi_i + \eta},$$
$$\hat{T}^E \approx \frac{2\,\mu_r \cos \varphi_i}{\mu_r \cos \varphi_i + \eta}. \tag{4.8}$$

For low frequencies, $\eta \gg 1$. Hence, $\hat{R}^E \approx -1$, and $\hat{T}^E \approx 0$.
Notice that with using the low-frequency approximation, all quantities have become independent on ϵ.

4.2 High-frequency/low-loss approximation

In the same way as in section 4.1, some useful approximations can be made for high frequencies. The high-frequency approximation is valid if $\frac{\sigma}{\omega\,\epsilon} \ll 1 - \frac{1}{\epsilon_r \mu_r} \sin^2\varphi_i$. Using a first order approximation for the index of refraction, η simplifies to

$$\eta \approx \sqrt{\epsilon_r \mu_r}\,\left(1 + \frac{\sigma}{2i\omega\epsilon}\right). \tag{4.9}$$

The propagation constant k_z is given by

$$k_z \approx \frac{\cos\varphi_t}{v}\left(\omega + \frac{\sigma}{2i\epsilon}\,\frac{1}{\cos^2\varphi_t}\right), \tag{4.10}$$

which yields for the skin depth

$$\delta \approx \frac{2\epsilon_0 c_0}{\mu_r \sigma}\sqrt{\epsilon_r \mu_r - \sin^2\varphi_i} = 2\sqrt{\frac{\epsilon}{\mu}}\,\frac{\cos\varphi_t}{\sigma}. \tag{4.11}$$

Notice that the skin depth has become frequency-independent.
After substitution of eq.(4.9) in (3.6), we obtain for the propagation factor

$$e^{-i(xk_x + zk_z)} \approx e^{-z/\delta}\, e^{-i\frac{\omega}{v}(x\sin\varphi_t + z\cos\varphi_t)}. \tag{4.12}$$

Also using the high-frequency approximation, the TM-mode reflection and

transmission coefficients can be written as

$$\hat{R}^H \approx \frac{\epsilon_r \cos\varphi_i - \sqrt{\epsilon_r\mu_r - \sin^2\varphi_i}}{\epsilon_r \cos\varphi_i + \sqrt{\epsilon_r\mu_r - \sin^2\varphi_i}} = \frac{1-\nu}{1+\nu},$$

(4.13)

$$\hat{T}^H \approx \frac{2\epsilon_r \cos\varphi_i}{\epsilon_r \cos\varphi_i + \sqrt{\epsilon_r\mu_r - \sin^2\varphi_i}} = \frac{2}{1+\nu},$$

with ν given by

$$\nu = (\mu_r/\epsilon_r)^{1/2} \frac{\cos\varphi_t}{\cos\varphi_i}. \tag{4.14}$$

The TE-mode reflection and transmission coefficients are in this case given by

$$\hat{R}^E \approx \frac{\mu_r \cos\varphi_i - \sqrt{\epsilon_r\mu_r - \sin^2\varphi_i}}{\mu_r \cos\varphi_i + \sqrt{\epsilon_r\mu_r - \sin^2\varphi_i}} = \frac{1-\rho}{1+\rho},$$

(4.15)

$$\hat{T}^E \approx \frac{2\mu_r \cos\varphi_i}{\mu_r \cos\varphi_i + \sqrt{\epsilon_r\mu_r - \sin^2\varphi_i}} = \frac{2}{1+\rho},$$

with ρ given by

$$\rho = (\epsilon_r/\mu_r)^{1/2} \frac{\cos\varphi_t}{\cos\varphi_i}. \tag{4.16}$$

Thus, when the high-frequency approximation can be used, we can make the following observations for both time and frequency domain as well as TM- and TE-mode. The reflected waves correspond to the lossless case, i.e.

as if $\sigma = 0$. The transmitted waves are also equal to those of the lossless case, except that there is a position-dependent attenuation with a factor $e^{-z/\delta}$.

5 SCATTERING OF A NEMP

In this chapter results are presented for an incident Nuclear ElectroMagnetic Pulse (NEMP). The NEMP is a transient signal with a very-short rise time of about 5 nsec and a large electric field strength with a peak value of 50 kV/m. Because of the short rise time the spectrum of the NEMP stretches up to 200 MHz.

5.1 Definition of the NEMP

Usually, the NEMP is approximated by a double exponential function given by

$$E_0(t) = A\,(e^{-\alpha t} - e^{-\beta t}), \tag{5.1}$$

with

$$\begin{aligned} A &= 5.278 \times 10^{4} \quad [\tfrac{V}{m}], \\ \alpha &= 3.705 \times 10^{6} \quad [s^{-1}], \\ \beta &= 3.908 \times 10^{8} \quad [s^{-1}]. \end{aligned} \tag{5.2}$$

The corresponding spectrum is given by

$$\hat{E}_0(i\omega) = A\left(\frac{1}{i\omega+\alpha} - \frac{1}{i\omega+\beta}\right). \tag{5.3}$$

Fig. 5.1 shows the wave form and the spectrum of the NEMP.

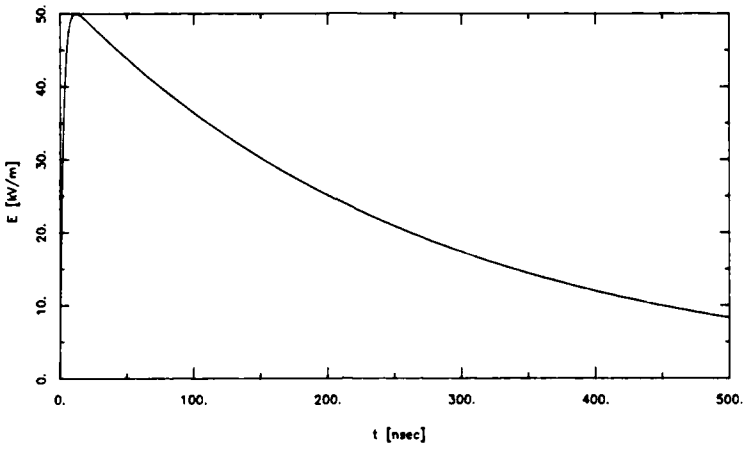

(a)

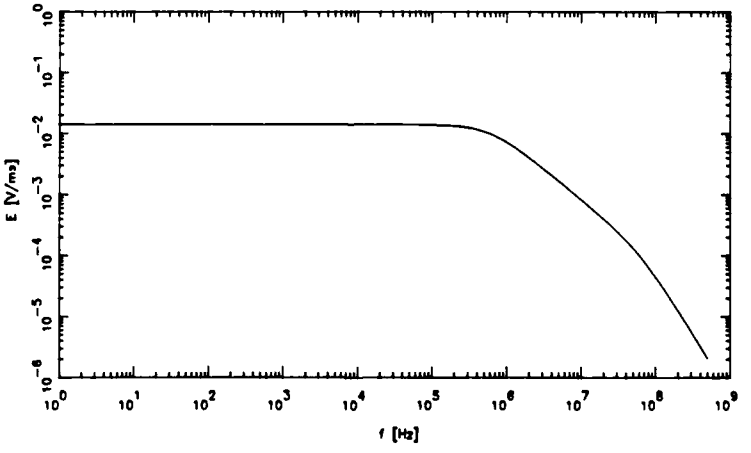

(b)

Fig. 5.1. Double exponential model for a NEMP.
a) wave form,
b) amplitude spectrum.

5.2 Scattering of the NEMP by the earth's surface

The constitutive constants ϵ and σ of the earth depend strongly on the structure and the kind of the soil. Table 5.1 gives an overview of some typical soils.

soil	ϵ_r []	σ [S/m]	$f = \sigma/2\pi\epsilon$ [MHz]
Humid soil, Clay	30	0.01-0.02	6
Fertile cultivated	15	0.005	6
Grass, Meadow	3.6	0.05-0.11	252
Dry soil	4	0.01	45

Table 5.1. Constitutive parameters of some typical soils.

For all soils listed in table 5.1 the relative permeability $\mu_r = 1$. The last column in table 5.1 gives the frequency f for which $f = \sigma/2\pi\epsilon$. Therefore, the low-frequency approximation is valid for all frequencies much smaller than the values listed in this column. From fig.5.1b one can see that for all of these values the incident NEMP does still contain a considerable amount of energy, so that the low-frequency approximation may not be applied for the frequencies that are contained in the NEMP.
Figs. 5.2-5.4 show the scattered field strength in the frequency and the time domain. The incident field is assumed to be a horizontally polarized NEMP.

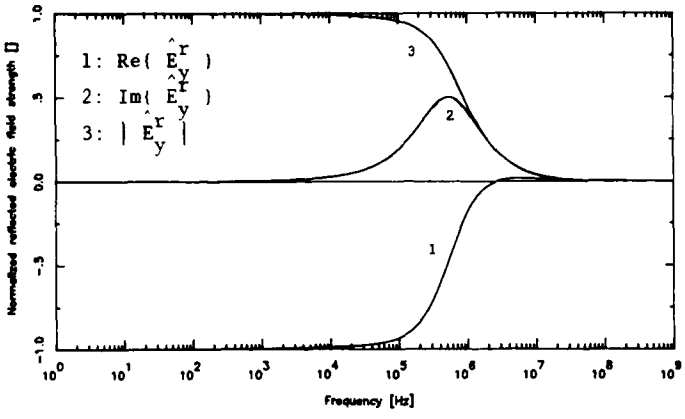

(a)

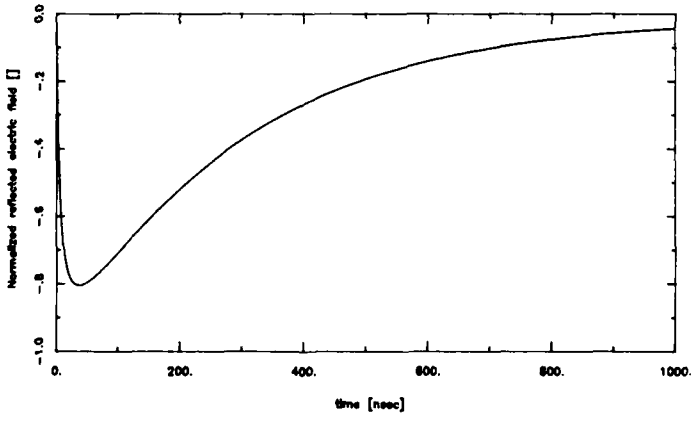

(b)

Fig.5.2. Reflected electric field strength for dry soil, $\epsilon_r = 4$, $\sigma = 10^{-2}$, $\mu_r = 1$. Horizontally polarized incident NEMP, $\varphi_i = 0^\circ$.
a) frequency domain ($1 \triangleq \hat{E}_0(0) = 1.41\times10^{-2}\ \frac{V}{m}\ s^{-1}$),
b) time domain ($1 \triangleq 50$ kV/m).

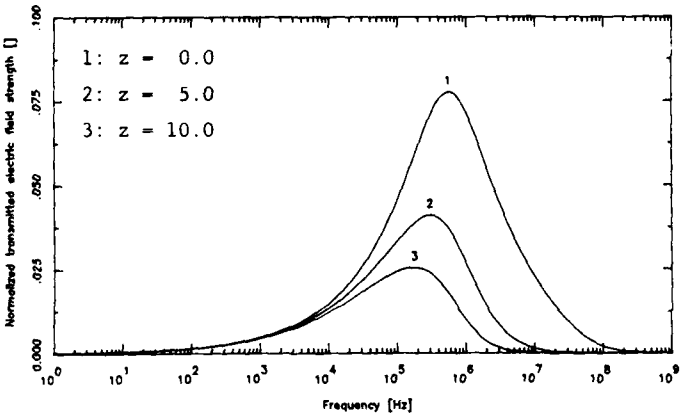

(a)

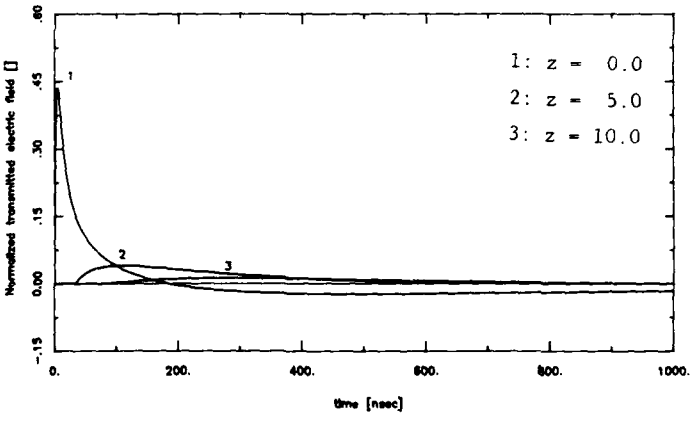

(b)

Fig.5.3. Transmitted electric field strength for dry soil, $\epsilon_r = 4$, $\sigma = 10^{-2}$, $\mu_r = 1$, at z = 0, 5, 10 m. Horizontally polarized incident NEMP, $\varphi_i = 0^\circ$.
a) frequency domain ($1 \triangleq \hat{E}_0(0) = 1.41\times10^{-2} \frac{V}{m} s^{-1}$),
b) time domain ($1 \triangleq 50$ kV/m).

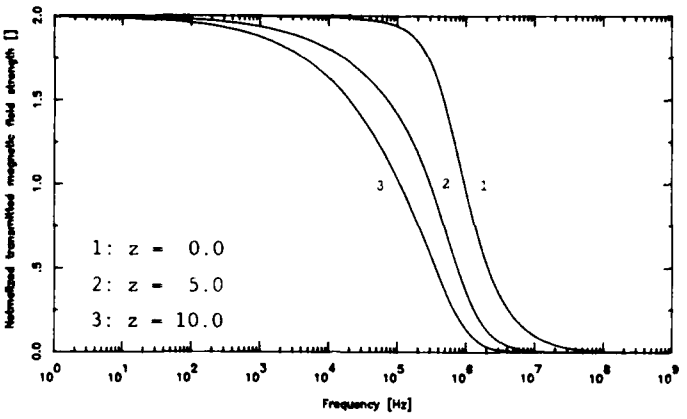

(a)

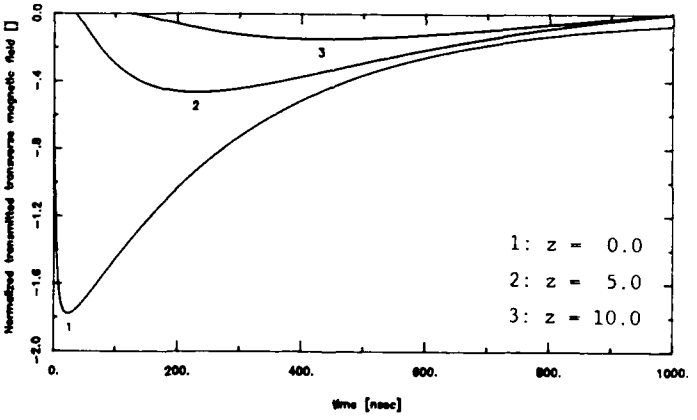

(b)

Fig.5.4. Transmitted magnetic field strength for dry soil, $\epsilon_r = 4$, $\sigma = 10^{-2}$, $\mu_r = 1$, at z = 0, 5, 10 m. Horizontally polarized incident NEMP, $\varphi_i = 0^\circ$.
a) frequency domain ($1 \triangleq Y_0 \hat{E}_0(0) = 3.74\times10^{-5} \frac{A}{m} s^{-1}$),
b) time domain ($1 \triangleq 132$ A/m).

The time-domain results were obtained by applying a 1024 points inverse Fast Fourier Transform (FFT), with a sampling frequency of 1 MHz. From fig.5.3 and 5.4 one can clearly observe that the high-frequency components of the transmitted fields are attenuated with increasing depth z. This is the effect of the skin depth δ, which decreases for high frequencies.

5.3 Scattering of a NEMP by water

The constitutive constants of sea and fresh water differ considerably. See table 5.2.

	ϵ_r []	σ [S/m]	$f = \sigma/2\pi\epsilon$ [MHz]
Sea water	80	1-5	1100
Fresh water	80	0.001-0.1	22

Table 5.2. Constitutive parameters of water, $\mu_r = 1$.

Because of the relative large conductivity σ of sea water, it can be considered as a good conductor for the frequencies of interest. This observation is supported by the last column of table 5.2, which again lists the frequency f given by $f = \sigma/2\pi\epsilon$. Therefore, if the incident NEMP is scattered by sea water the low-frequency/high-loss approximation can be used for all frequencies of the NEMP spectrum.

From the low-frequency/high-loss approximation, we conclude that a horizontally polarized incident NEMP is reflected almost totally by sea water, with a phase change of 180° (recall $R^E \approx -1$). Now the electric field strength $\hat{E}^t = \|\underline{\hat{E}}^t\|$ just beneath the surface, is given by

$$\hat{E}^t = \left(\frac{2\omega\epsilon_0}{\sigma} \right)^{1/2} (1 + i) \cos \varphi_i \, \hat{E}^i, \qquad z \downarrow 0 \tag{5.4}$$

where $\hat{E}^i$ denotes the field strength of the incident field, i.e. $\hat{E}^i = \|\underline{\hat{E}}^i\| = \hat{E}^i_y$. Since $\sigma/\omega\epsilon \gg 1$, it follows that the electric field strength just beneath the surface, is small compared with the incident electric field strength.
The magnetic field strength $\hat{H}^t = \|\underline{\hat{H}}^t\|$ just beneath the surface, is given by

$$\hat{H}^t = \frac{\gamma}{i\omega} \hat{E}^t \quad Y\,(1 + \frac{\sigma}{i\omega\epsilon})^{1/2}\,\hat{E}^t, \qquad z \downarrow 0 \tag{5.5}$$

where Y denotes the dielectric impedance of the medium in $\mathcal{D}_2$ given by

$$Y = (\epsilon/\mu)^{1/2}. \tag{5.6}$$

Using the relation $\hat{E}^t = \hat{T}^E \hat{E}^i$, we find after some simple manipulation

$$\hat{H}^t = 2 \cos \varphi_i \hat{H}^i. \tag{5.7}$$

Hence, the magnetic field strength can be twice the incident magnetic field strength.
For a vertically polarized incident NEMP, the reflection coefficient equals almost 1, and so the transmission coefficient equals almost 2. Therefore, the magnetic field just beneath the surface, is twice the value of the magnetic field strength of the incident field. The electric field strength $\hat{E}^t$ just beneath the surface, is given by

$$\hat{E}^t = \frac{\gamma}{i\omega\epsilon+\sigma} \hat{H}^t = (\frac{1}{1 + \frac{\sigma}{i\omega\epsilon}})^{1/2} Z \hat{H}^t, \qquad z \downarrow 0 \tag{5.8}$$

where Z denotes the dielectric impedance of the medium in $\mathcal{D}_2$ given by

$$Z = (\mu/\epsilon)^{1/2}. \tag{5.9}$$

Using the approximation $\hat{H}^t \approx 2\,\hat{H}^i$, we finally arrive at

$$\hat{E}^t = 2\,\epsilon_r^{-1/2}\left(\frac{1}{1+\frac{\sigma}{i\omega\epsilon}}\right)^{1/2}\hat{E}^i \qquad z\downarrow 0 \tag{5.10}$$

Since $\frac{1}{1+\frac{\sigma}{i\omega\epsilon}} \ll 1$, we can conclude from eq.(5.10) that the electric field strength in $\mathcal{D}_2$ is very small compared with the incident electric field strength.

From these arguments we can conclude that in the case of scattering by sea water, for both horizontal and vertical polarization, the electric field strength in $\mathcal{D}_2$ is relatively small compared with the incident electric field strength, while the magnetic field strength in $\mathcal{D}_2$, equals twice the incident magnetic field strength. However, the transmitted fields are attenuated rapidly for increasing depth z due to the skin depth δ.

Figs. 5.5-5.7 show the scattered field strengths for vertical polarization, both in the time and frequency domain. The time-domain results were obtained using a 1024 points inverse FFT. The sampling frequency was 1 MHz.

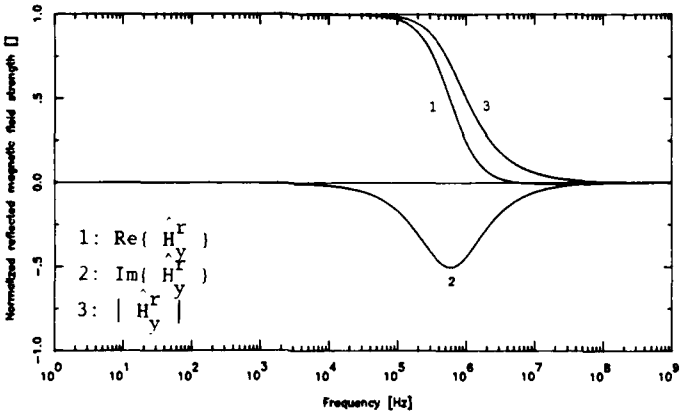

(a)

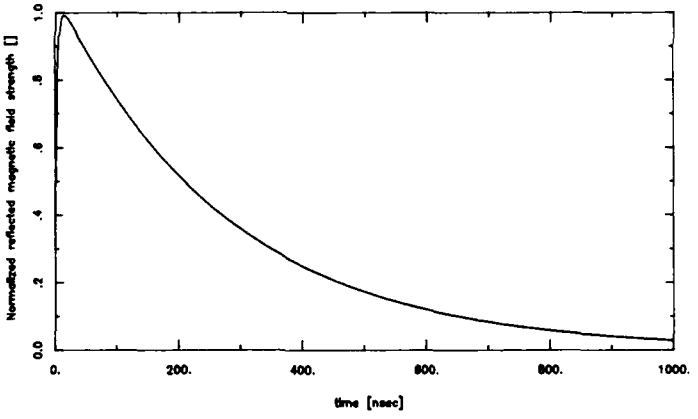

(b)

Fig.5.5. Reflected magnetic field strength from sea water (ϵ_r = 80, σ = 1, μ_r = 1). Vertically polarized incident NEMP, $\varphi_i = 0^\circ$.
a) frequency domain ($1 \triangleq \hat{Y}_0\hat{E}_0(0) = 3.74\times10^{-5}\ \frac{A}{m}\ s^{-1}$),
b) time domain ($1 \triangleq 132$ A/m).

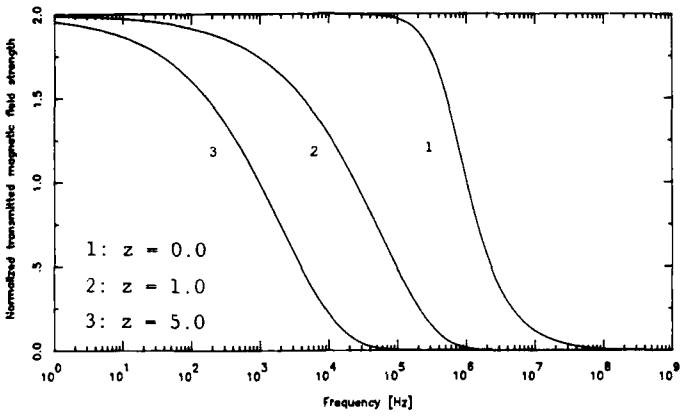

(a)

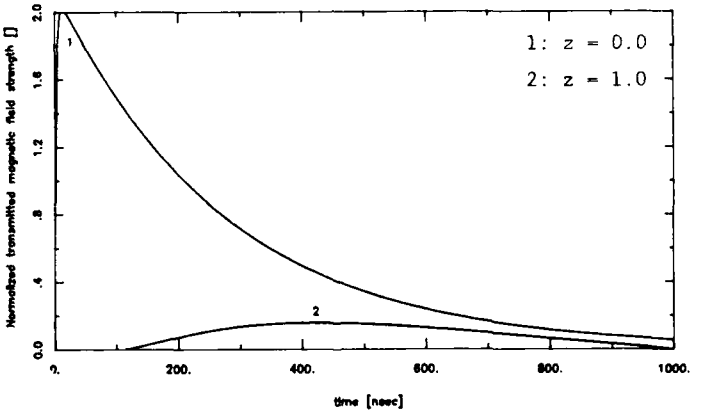

(b)

Fig.5.6. Transmitted magnetic field strength from sea water (ϵ_r = 80, σ = 1, μ_r = 1), at z = 0, 1, 5 m. Vertically polarized incident NEMP, $\varphi_i = 0^\circ$.
a) frequency domain ($1 \triangleq Y_0 \hat{E}_0(0) = 3.74\times10^{-5}\ \frac{A}{m}\ s^{-1}$),
b) time domain ($1 \triangleq 132$ A/m).

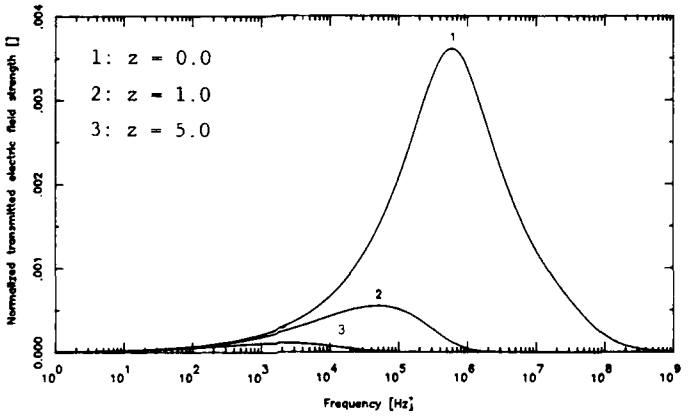

(a)

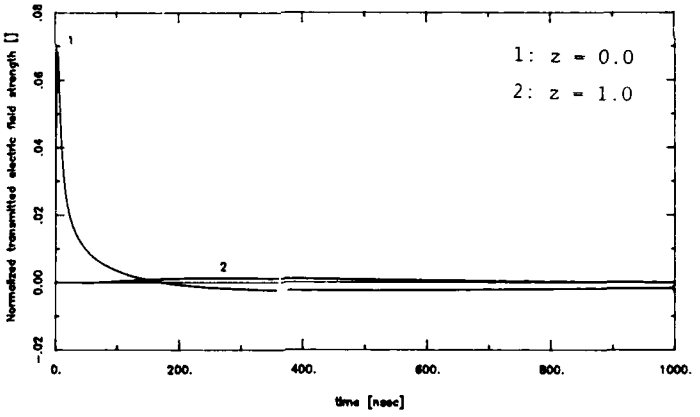

(b)

Fig.5.7. Transmitted electric field strength from sea water (ϵ_r = 80, σ = 1, μ_r = 1), at z = 0, 1, 5 m. Vertically polarized incident NEMP, $\varphi_i = 0^\circ$.
a) frequency domain ($1 \triangleq \hat{E}_0(0) = 1.41\times10^{-2}\ \frac{V}{m}\ s^{-1}$),
b) time domain ($1 \triangleq$ 50 kV/m).

6 CONCLUSIONS

The expressions for the scattered electromagnetic fields can be approximated using the low-frequency/high-loss or high-frequency/low-loss approximation. It was shown that the spectrum of the NEMP is such that only in the case of scattering by sea water the low-frequency/high-loss approximation can be used. In all other cases no approximations are allowed, that is if the exact solution of the scattering process is searched for.
It was also shown that in the case of scattering by sea water and if the amplitude spectrum of the incident field is such that the low-frequency/high-loss approximation may be applied, the transmitted magnetic field strength can be twice the value of the incident field strength. In this case the transmitted electric field strength is very small compared to the incident electric field strength.

The analysis and results of the previous chapters where performed in the Laplace or frequency domain. Time-domain results can be obtained by applying the inverse Fast Fourier Transform (FFT) numerically to the expressions for the reflected and transmitted waves.
Although the expressions for the scattered electromagnetic fields are rather complicated, it is believed that time-domain expressions can be arrived. This is a subject of further research.

p.o.

Ir R. Middelkoop
(EMP group leader)

Ir J.J.A. Klaasen
(author)

REFERENCES

[1] LePage, W.R., Complex Variables and the Laplace Transform for Engineers, McGraw-Hill Book Company, Inc., 1961, pp. 318 - 320

[2] Wait, J.R., Electromagnetic Waves in Stratified Media, Pergamon Press, 1960, pp. 10 - 21

[3] Stratton, J.A., Electromagnetic Theory, McGraw-Hill Book Company, Inc., 1941, pp. 490 - 511

[4] Collin, R.E., Field Theory of Guided Waves, McGraw-Hill Book Company, Inc., 1960, pp. 76 - 96

UNCLASSIFIED

REPORT DOCUMENTATION PAGE (MOD-NL)

1. DEFENSE REPORT NUMBER (MOD-NL)	2. RECIPIENT'S ACCESSION NUMBER	3. PERFORMING ORGANIZATION REPORT NUMBER
TD90-1714		FEL-90-A112
4. PROJECT/TASK/WORK UNIT NO.	**5. CONTRACT NUMBER**	**6. REPORT DATE**
5168	A86K012	MAY, 1990
7. NUMBER OF PAGES	**8. NUMBER OF REFERENCES**	**9. TYPE OF REPORT AND DATES COVERED**
42	4	FINAL REPORT

10. TITLE AND SUBTITLE
FREQUENCY-DOMAIN ANALYSIS OF ONE-DIMENSIONAL ELECTROMAGNETIC SCATTERING BY LOSSY MEDIA

11. AUTHOR(S)
IR. J.J.A. KLAASEN

12. PERFORMING ORGANIZATION NAME(S) AND ADDRESS(ES)
TNO PHYSICS AND ELECTRONICS LABORATORY
POBOX 96864, 2509 JG THE HAGUE, THE NETHERLANDS

13. SPONSORING/MONITORING AGENCY NAME(S)

14. SUPPLEMENTARY NOTES
IN ENGLISH

15. ABSTRACT (MAXIMUM 200 WORDS, 1044 POSITIONS)
A STUDY WAS PERFORMED TO INVESTIGATE THE EFFECT OF A PLANE INTERFACE BETWEEN TWO MEDIA WITH DIFFERENT ELECTROMAGNETIC PROPERTIES, ON THE ELECTROMAGNETIC FIELDS. SUCH AN INTERFACE EXISTS BETWEEN E.G. AN AIR/EARTH OR AIR/WATER BOUNDARY. THIS REPORT PRESENTS THE RESULTS OF THIS STUDY.
THE INCIDENT FIELD IS ASSUMED TO BE A UNIFORM PLANE WAVE. THEREFORE THIS STUDY ADRESSES THE ONE-DIMENSIONAL SCATTERING PROBLEM. THE ANALYSIS IS PERFORMED IN THE S-DOMAIN, I.E. USING THE LAPLACE TRANSFORM.
NUMERICAL RESULTS ARE PRESENTED FOR THE SCATTERING OF A NEMP BY THE EARTH'S SURFACE AND THE SEA.

16. DESCRIPTORS	IDENTIFIERS
ELECTROMAGNETIC PULSE	EMP
NUMERICAL CALCULATIONS	
SCATTERING OF ELECTROMAGNETIC WAVES	
FRESNEL REFLECTION, REFRACTION	

17a. SECURITY CLASSIFICATION (OF REPORT)	17b. SECURITY CLASSIFICATION (OF PAGE)	17c. SECURITY CLASSIFICATION (OF ABSTRACT)
UNCLASSIFIED	UNCLASSIFIED	UNCLASSIFIED

18. DISTRIBUTION/AVAILABILITY STATEMENT	17d. SECURITY CLASSIFICATION (OF TITLES)
UNLIMITED AVAILABILITY	UNCLASSIFIED

UNCLASSIFIED